

Running title: PTHR1 signaling in osteocytes and cortical bone

Y Rhee: yumie@yuhs.ac

MR Allen: matallen@iupu.edu

K Condon: kcondon@iupui.edu

V Lezcano: vlezcano@criba.edu.ar

AC Ronda: acronda@criba.edu.ar

N Olivos: nolivos@toromail.csudh.edu

C Galli: carlo.galli@unipr.it

G Passeri: giovanni.passeri@unipr.it

CA O'Brien: obriencharlesa@uams.edu

N Bivi: nicobivi@iupui.edu

LI Plotkin: lplotkin@iupui.edu

*Corresponding author: Teresita Bellido, Ph.D. Department of Anatomy and Cell Biology, and Department of Internal Medicine, Division of Endocrinology, Indiana University School of Medicine, 635 Barnhill Drive, MS5035, Indianapolis, IN 46202. Phone 317-274-7410; Fax 317-278-2040. tbellido@iupui.edu

Funding sources: This research was supported by the National Institutes of Health (R01 DK076007, S10-RR023710, P01 AG13918, TW06919, GM067592).

Conflict of interest: The authors declare that no conflict of interest exists

Abstract

The periosteal and endocortical surfaces of cortical bone dictate the geometry and overall mechanical properties of bone. Yet, the cellular and molecular mechanisms that regulate activity on these surfaces are far from being understood. Parathyroid hormone (PTH) has profound effects in cortical bone, stimulating periosteal expansion and at the same time accelerating intra-cortical bone remodeling. We report herein that transgenic mice expressing a constitutive active PTH receptor in osteocytes (DMP1-caPTH1 mice) exhibit increased cortical bone area and elevated rate of periosteal and endocortical bone formation. In addition, DMP1-caPTH1 mice display marked increase in intra-cortical remodeling and cortical porosity. Crossing DMP1-caPTH1 mice with mice lacking the Wnt co-receptor LDL related receptor 5 (LRP5) or with mice overexpressing the Wnt antagonist Sost in osteocytes (DMP1-Sost mice), reduced or completely abolished, respectively, the increased cortical bone area, periosteal BFR, and expression of osteoblast markers and Wnt target genes exhibited by the DMP1-caPTH1 mice. In addition, DMP1-caPTH1 lacking LRP5 or double transgenic DMP1-caPTH1;DMP1-Sost mice exhibit exacerbated intra-cortical remodeling and osteoclast numbers, and markedly decreased expression of the RANK decoy receptor osteoprotegerin (OPG). Thus, whereas Sost downregulation and the consequent Wnt activation is required for the stimulatory effect of PTH receptor signaling on periosteal bone formation, the Wnt-independent increase in osteoclastogenesis induced by PTH receptor activation in osteocytes overrides the effect on Sost. These findings demonstrate that PTH receptor signaling influences cortical bone through actions on osteocytes and define the role of Wnt signaling in PTH receptor action.

Key words: osteocytes, PTH receptor, periosteal bone formation, Wnt signaling, intra-cortical remodeling

Introduction

The skeleton is composed of cancellous or trabecular bone intertwined with bone marrow surrounded by a shell of cortical bone. Bone formation on the periosteal surface of cortical bone regulates the outer shape of bones and, in concert with activity on the endocortical surface, determines cortical thickness and bone size. Periosteal expansion significantly increases bone strength, independently of increases in areal bone mineral density ^(1,2). Fractures in clinically relevant sites initiate in the cortical bone ⁽³⁾, even in bones composed predominantly of cancellous bone such as the femoral neck ⁽⁴⁾. Moreover, greater cortical bone mass may explain the higher resistance to vertebral fracture in males compared to females ^(5,6). Despite the influence of cortical bone, and specifically the periosteum, on fracture prevention, the mechanisms that govern cortical bone biology and the response of this site to osteoporotic therapies are far from being understood.

Mechanical and hormonal stimuli influence periosteal bone formation during growth as well as in the adult skeleton ⁽⁷⁾. In particular, parathyroid hormone (PTH) is a key stimulator of periosteal expansion ⁽⁸⁾. Early studies in humans showed that asymptomatic patients with either primary hyperparathyroidism or hyperparathyroidism secondary to chronic kidney disease exhibit increased metacarpal outer diameter ⁽⁸⁾. Consistent with this, patients with primary hyperparathyroidism exhibit 2-3-fold higher periosteal bone formation rate (BFR) than controls ⁽⁹⁾. Daily injections of PTH to osteoporotic patients also augment cortical bone width and increase BFR on both periosteal and endocortical surfaces ⁽¹⁰⁾. In rodents and rabbits, intermittent PTH administration enhances periosteal bone formation ⁽¹¹⁻¹⁴⁾, by a mechanism that might

require insulin-like growth factor 1 signaling ^(15,16). All this evidence notwithstanding, elevation of PTH not always increases bone formation on the periosteal surface ⁽¹⁷⁻¹⁹⁾.

The bases for this apparent dichotomy are not understood.

In cancellous bone, PTH increases bone formation by mechanisms that seem to differ depending on the mode of elevation. The anabolic effect of intermittent PTH in rodents can be accounted for by prolonging the life span of mature osteoblasts in combination with pro-differentiating effects of the hormone ⁽²⁰⁻²²⁾; whereas chronic elevation of PTH increases osteoblast number by acting on osteocytes to suppress the expression of the bone formation inhibitor sclerostin, encoded by the *Sost* gene ^(23,24). Recent evidence demonstrate that transgenic mice expressing a constitutively active PTH receptor 1 exclusively in osteocytes (DMP1-caPTHR1 mice) exhibit reduced sclerostin expression, increased Wnt signaling, and increased cancellous bone volume ⁽²⁵⁾. In addition, these mice display elevated bone turnover markers. These findings suggest that previously unrecognized effects of PTH on osteocytes mediate at least some of the actions of the hormone on the skeleton. Whether PTH regulates cortical bone by acting on osteocytes had remained unknown.

We report here that osteocyte-specific constitutive activation of the PTH receptor leads to increased cortical bone area and elevated rate of periosteal and endocortical bone formation. In addition, DMP1-caPTHR1 mice display a remarkable increase in intra-cortical remodeling associated with increased cortical porosity. Removal of the Wnt co-receptor LDL related receptor 5 (LRP5) or osteocyte-targeted overexpression of *Sost*, whose product sclerostin binds to both LRP5 and 6, reduced or completely abolished, respectively, the increased cortical bone area, periosteal BFR, and expression of

osteoblast markers and Wnt target genes exhibited by the DMP1-caPTH_{R1} mice. In addition, interference with the Wnt pathway exacerbated intra-cortical remodeling and the increase in osteoclast number displayed by the DMP1-caPTH_{R1} mice and markedly decreased the expression of the RANK decoy receptor osteoprotegerin (OPG). These findings demonstrate that PTH receptor signaling influences cortical bone through actions on osteocytes and define the role of Wnt signaling in PTH receptor action.

Materials and Methods

Generation of DMP1-caPTH_{R1} and DMP-Sost transgenic mice and crosses with LRP5^{-/-} mice or DMP1-Sost mice

Generation of DMP1-caPTH_{R1} transgenic mice was described previously ⁽²⁵⁾. DMP1-Sost transgenic mice were generated by inserting the human Sost cDNA (I.M.A.G.E. clone ID: 40009482, American Tissue Culture Collection) downstream from a 12 kb DNA fragment containing 8 kb of the 5'-flanking region, the first exon, the first intron, and 17 bp of exon 2 of the murine DMP1 gene ⁽²⁶⁾, and upstream from a 140 bp fragment containing the rabbit beta-globin polyadenylation sequence. Transgenic mice were produced by microinjection of purified DNA into pronuclei of C57BL/6 mice at the transgenic mouse core facility of the University of Arkansas for Medical Sciences. DMP1-Sost mice were born at the expected Mendelian frequency, were fertile, and exhibited normal size and weight. DMP1-caPTH_{R1} and DMP1-Sost mouse colonies were maintained by breeding mice hemizygous for the transgene with wild type C57BL/6 mice. All transgenic mice used in these studies were hemizygous. The DMP1-caPTH_{R1} and DMP1-Sost transgenes were detected in bone but not in skeletal muscle, heart, brain, kidney, duodenum or colon [⁽²⁵⁾ and **Supplementary Figures 1A and B**].

DMP1-caPTH_{R1} mice were crossed with mice lacking LRP5⁽²⁷⁾ or with DMP1-Sost mice to obtain mice expressing the DMP1-caPTH_{R1} transgene in a LRP5 deficient background or mice expressing both the DMP1-caPTH_{R1} and the DMP1-Sost transgenes. Animals were fed a regular diet (Harlan/Teklad #7001) and water ad libitum and maintained on a 12-h light/dark cycle. Animal protocols were approved by the Institutional Animal Care and Use Committees of the University of Arkansas for Medical Sciences and Indiana University School of Medicine.

Analysis of skeletal phenotypes

Analysis of the skeletal phenotypes was performed in mice of 4.6 to 12 week of age as detailed in the legend of each figure. Bone mineral density (BMD) was determined by dual energy x-ray absorptiometry (DXA) using a PIXImus II densitometer (G.E. Medical Systems) as previously described⁽²⁵⁾. Mice were anesthetized via inhalation of 2.5% isoflurane (Abbott laboratories) mixed with O₂ (1.5 liter/min). BMD measurements of the total body excluding the head, lumbar spine, and femur were taken. For micro-CT analysis, femora and L3 vertebra were dissected, cleaned of soft tissue, stored in 70% ethanol, and scanned at 6 micron resolution (Skyscan 1172, SkyScan). For histomorphometric analysis, femora and calvariae were dissected, fixed, and embedded in methyl methacrylate. Fluorochrome labeling of the bones was performed by intraperitoneal injections of calcein (30 mg/kg) and alizarin (50 mg/kg; Sigma Chemical) administered 7 and 2 days before sacrifice, respectively, as previously described⁽²⁵⁾. Thick cross-sections of undecalcified femora at the mid-diaphysis were prepared using a diamond embedded wire saw (Histosaw, Delaware Diamond Knives) and ground to a

final thickness of 30-35 μm . Frontal plane 8 μm -thick calvarial sections were obtained 2 mm anterior to the junction between fronto-parietal and sagittal sutures using an Automated Rotary Microtome Leica RM2255 (Leica Microsystems Inc.). Sections were viewed at 20-40 X magnification on a Leitz DMRXE microscope (Leica Mikroskopie und System GmbH). Images were captured using a SPOT digital camera (Diagnostic Instruments, Inc.). Total, single, and double labeled perimeter, and inter-label width were measured on periosteal and endocortical surfaces of 2 femoral sections per mouse and on outer and inner periosteal surfaces of 1 calvarial section per mouse, using a semiautomatic analysis system (Bioquant OSTEO 7.20.10, Bioquant Image Analysis Co.) attached to a microscope equipped with an ultraviolet light source (Nikon Optiphot 2 microscope). A combination of von Kossa to stain mineralized bone, followed by enzyme histochemistry for TRAPase, and counter-stain with Gill's III hematoxylin was used to visualize osteoclasts in calvarial sections ^(25,28). TRAPase positive multinucleated cells were enumerated using the OsteoMeasure High Resolution Digital Video System (OsteoMetrics, Inc.) attached to an Olympus BX51TRF microscope (Olympus America Inc.). Osteoclast number was expressed per bone area. The terminology and units used are those recommended by the Histomorphometry Nomenclature Committee of the American Society for Bone and Mineral Research ⁽²⁹⁾.

Bone turnover markers

Plasma osteocalcin and C-telopeptide fragments of type I collagen (CTX) were measured using enzyme linked immunoadsorbent assays (Biomedical Technologies and Immunodiagnostic Systems Inc. respectively), as published ⁽²⁵⁾.

Immunohistochemistry

Detection of sclerostin expression on paraffin-embedded tibiae from 6-week-old mice was performed as previously described^(24,25). Briefly, sections were deparaffinized, treated with 3% H₂O₂ to inhibit endogenous peroxidase activity, blocked with rabbit or goat serum, and then incubated with 1:100 dilution of goat polyclonal anti-mouse sclerostin antibody (R&D Systems) or rabbit polyclonal anti-human sclerostin antibody (Abcam Inc.), respectively. Sections were then incubated with rabbit anti-goat horseradish peroxidase-conjugated secondary antibody (Santa Cruz Biotechnologies) or goat anti-rabbit biotinylated secondary antibody followed by avidin conjugated peroxidase (Vectastain Elite ABC Kit; Vector Laboratories). Color was developed with a diaminobenzidine substrate chromogen system (Dako Corp.). Non-immune IgGs were used as negative controls.

Quantitative PCR

Whole tibiae from 12-week-old DMP1-caPTH^{R1};LRP5^{-/-} mice or ulnae from 6-week-old DMP1-caPTH^{R1};DMP1-Sost mice were snap frozen at sacrifice. Total RNA was purified using Ultraspec reagent (Biotecx Laboratories) according to the manufacturer's instructions. Gene expression was analyzed by quantitative PCR as previously described⁽²⁵⁾ using primer probe sets from Applied Biosystems or from Roche Applied Science. Relative mRNA expression levels were normalized to the house-keeping gene ribosomal protein S2 using the Δ Ct method.

Statistical analysis

Data were analyzed using SigmaStat (SPSS Science). All values are reported as the mean \pm standard deviations (SD). Differences between group means were evaluated using Student's t-test or two-way ANOVA.

Results

Mice expressing a constitutively active PTHR1 in osteocytes exhibit increased cortical bone area, and elevated periosteal and endocortical bone formation.

Microscopic examination of cross-sectional cuts of the femur at mid-diaphysis of 4.6-week-old mice showed larger bone diameter in DMP1-caPTHR1 bones (**Figure 1A**).

Histomorphometric analysis showed that the total cross-sectional area was 17% higher and cortical thickness and cortical bone area approximately double in the DMP1-caPTHR1 mice (**Figure 1B**). These geometry differences resulted from enhanced activity on both cortical surfaces and, whereas wild type (WT) littermate midshafts exhibited the classical pattern of modeling with fluorochrome labeling present only in part of the periosteal and the opposite endocortical surfaces, fluorochrome incorporation in DMP1-caPTHR1 bones was observed along the entire periosteal and endocortical surfaces (**Figure 1A**). Mineralizing surface per bone surface (MS/BS) was markedly increased in the periosteal and endocortical surface of DMP1-caPTHR1 mid-diaphyses compared to WT littermates. Mineral apposition rate (MAR) was also increased in both periosteal and endocortical surfaces, although the effect was only statistically significant in the periosteum (**Figure 1B**). This resulted in a significant increase in periosteal and

endocortical BFR on both surfaces in DMP1-caPTH_{R1} mice. Similar changes were found in male and female mice.

We next examined the periosteal surface in the compact bone of the skull, which is formed by intramembranous ossification (**Figure 2**). BFR measured on both the outer and inner calvarial periosteal surface was also higher in the DMP1-caPTH_{R1} mice. Calvarial thickness measured in transverse sections was 1.4-fold higher in DMP1-caPTH_{R1} mice.

DMP1-caPTH_{R1} mice exhibit increased bone remodeling in cortical bone. Previous histomorphometric analysis of cancellous bone at the distal femur of DMP1-caPTH_{R1} indicated that not only osteoblast but also osteoclast perimeter was elevated and quiescent surface was decreased ⁽²⁵⁾. We also found abundant fluorochrome incorporation, an index of intra-cortical (endosteal) bone formation, in cortical bone at the femoral diaphysis (**Figure 1A**) as well as in calvaria (**Figure 2A**) of DMP1-caPTH_{R1} mice. In addition, calvarial porosity measured histomorphometrically as marrow area per bone area was observed only in calvariae of the DMP1-caPTH_{R1} mice (**Figure 2C**). In addition, abundant osteoclasts were present only in DMP1-caPTH_{R1} calvaria (**Figure 2D**). Taken together with the previous findings that plasma and urine markers of bone resorption are elevated in these mice ⁽²⁵⁾, we conclude that activation of PTH receptor signaling in osteocytes leads to increased bone remodeling in cortical as well as cancellous bone.

The periosteal bone phenotype of the DMP1-caPTH1 mice is partially reversed in the absence of LRP5 and abolished by Sost overexpression. Previous findings had shown that the increased cancellous bone of the DMP1-caPTH1 mice was reduced in mice also lacking the Wnt co-receptor LRP5 ⁽²⁵⁾. To examine whether a similar mechanism was involved in the effect of the DMP1-caPTH1 transgene on cortical bone, we analyzed the femoral mid-diaphysis of the DMP1-caPTH1 mice crossed with LRP5^{-/-} mice. As shown for younger mice in **Figure 1**, 3-month-old DMP1-caPTH1 exhibited increased cross-sectional area, cortical thickness, and cortical bone area (**Figure 3A and B**). The increase in these parameters was significantly reduced, but not eliminated, in DMP1-caPTH1 mice lacking LRP5. Similarly, the higher periosteal BFR and mineralizing surface observed even in these 3-month-old DMP1-caPTH1 mice was partially reversed in the absence of LRP5 (**Figure 3C**). At this age, however, the effect of the DMP1-caPTH1 transgene on the endocortical surface did not reach significance (**Figure 3D**).

The persistent effect of the DMP1-caPTH1 transgene on cortical bone in LRP5 deficient mice might result from remaining increased Wnt signaling through LRP6. Sclerostin interacts with and inhibits signaling through both LRP5 and 6 ⁽³⁰⁾. To directly address the role of suppressed Sost/sclerostin expression in the actions of the caPTH1, we generated mice overexpressing the human Sost gene in osteocytes (DMP1-Sost mice) and crossed them with DMP1-caPTH1 mice. Expression of human Sost mRNA was only found in DMP1-Sost mice, whereas endogenous murine Sost was detected at similar levels in mice expressing or not the DMP1-Sost transgene (**Figure**

4A). Mice expressing the DMP1-caPTH1R1 transgene exhibited decreased expression of endogenous murine Sost, regardless of whether the DMP1-Sost transgene was expressed or not. Immunohistochemistry using an antibody against murine sclerostin that also recognizes the human protein, demonstrated sclerostin expression in osteocytes in bone sections of WT and DMP1-Sost mice (**Figure 4B**). Consistent with previous findings ⁽²⁵⁾, sclerostin expression was markedly decreased in osteocytes of DMP1-caPTH1R1 mice. On the other hand, DMP1-caPTH1R1 mice co-expressing the DMP1-Sost transgene exhibited persistent high expression of sclerostin (**Figure 4B**, upper panel). Although mRNA for the human Sost transgene was expressed at lower levels in animals co-expressing the DMP1-caPTH1R1 transgene, human sclerostin detected using anti-human sclerostin antibody was detectable in both DMP1-Sost mice expressing or not expressing the DMP1-caPTH1R1 transgene (**Figure 4B**, lower panel).

BMD measurements taken at 4, 6 (not shown), and 8 (**Figure 4C**) weeks of age revealed no significant change in total or femoral BMD in DMP1-Sost mice. However, spinal BMD was significantly lower at all ages (**Figure 4C** and not shown). Micro-CT analysis showed no changes in cortical bone area in the femoral mid-diaphyses but a dramatic decrease in cancellous bone volume in the vertebrae of DMP1-Sost mice (**Figure 4D**). Despite this apparent differential effect of the DMP1-Sost transgene on cortical and cancellous bone, the increase in BMD exhibited by DMP1-caPTH1R1 mice was completely abolished at both the femur and spine in mice expressing both DMP1-caPTH1R1 and the DMP1-Sost transgenes (**Figure 4C** and **D**). Furthermore, the double-transgenic mice exhibited significantly lower BMD in all sites than mice expressing

solely the DMP1-Sost transgene (**Figure 4C and D**), due to increased osteoclast activity as it will be discussed below.

In contrast to the incomplete effect of deleting LRP5, the higher cortical bone area exhibited by the DMP1-caPTH1 mice was completely eliminated in mice also expressing the DMP1-Sost transgene (**Figure 5**). Thus, total cross-sectional area, cortical thickness, cortical bone area, and periosteal BFR in the double-transgenic mice were similar to those observed in DMP1-Sost mice or in non-transgenic mice. Sost overexpression also reduced the increased thickness and periosteal bone formation induced by the DMP1-caPTH1 transgene in calvaria (**Supplementary Figure 2**).

The elevated intra-cortical bone remodeling exhibited by the DMP1-caPTH1 mice is still present in the absence of LRP5 and it is exacerbated by Sost overexpression. Despite the lower periosteal bone formation induced by the DMP1-caPTH1 transgene in LRP5^{-/-} mice or in mice overexpressing Sost in osteocytes, DMP1-caPTH1;LRP5^{-/-} and DMP1-caPTH1;DMP1-Sost mice displayed persistently higher intra-cortical remodeling resembling DMP1-caPTH1 mice (**Figure 6**). Thus, abundant intra-cortical fluorochrome incorporation was still observed in sections of femoral mid-diaphysis and calvaria (**Figures 3, S2, and Figure 5**). Calvarial marrow space was similarly higher in DMP1-caPTH1 mice lacking or expressing LRP5 (**Figure 6A**); and double transgenic DMP1-caPTH1;DMP1-Sost mice exhibited even higher calvarial marrow space compared to mice expressing only the DMP1-caPTH1 transgene. Osteoclast number per bone area quantified in vonKossa/TRAPase calvarial sections displayed similar profile (**Figure 6B**). Circulating levels of both formation (osteocalcin) and resorption (CTX) markers were increased in DMP1-caPTH1 mice.

CTX was still elevated in DMP1-caPTH^{R1};DMP1-Sost mice (**Figure 6C**). However, osteocalcin levels in DMP1-caPTH^{R1};DMP1-Sost mice were significantly lower than in DMP1-caPTH^{R1} mice (**Figure 6C**), as previously shown for DMP1-caPTH^{R1};LRP5^{-/-} mice ⁽²⁵⁾.

Interference with the Wnt pathway decreased the expression of Wnt target genes and osteoblast markers induced by PTH receptor activation in osteocytes, but osteoclastogenic cytokines and osteoclast markers remained increased. Long bones from DMP1-caPTH^{R1} mice exhibited increased expression of Wnt target genes as well as of osteoblast and osteoclast markers (**Figure 7**). Gene expression was remarkably affected in DMP1-caPTH^{R1} mice crossed with LRP5 null mice or with DMP1-Sost mice. Thus, the higher expression of the recognized Wnt target genes naked2, cyclin D1, Cx43, and BMP4 ^(25,31) observed in the DMP1-caPTH^{R1} mice was eliminated in mice also expressing the Sost transgene (**Figure 7A**). Naked2 expression was also decreased to WT values by deletion of LRP5. However, expression of cyclin D1 was barely affected, whereas Cx43 and BMP4 expression was reduced, although not eliminated, in DMP1-caPTH^{R1};LRP5^{-/-} mice. Consistent with the higher periosteal bone formation, the osteoblast markers alkaline phosphatase, collagen 1a1, and osteocalcin were elevated in DMP1-caPTH^{R1} mice (**Figure 7B**). Deletion of LRP5 did not affect alkaline phosphatase expression, decreased only partially collagen 1a1 expression, and completely block osteocalcin expression. Sost overexpression abolished the increases in all these genes exhibited by the DMP1-caPTH^{R1} mice.

In contrast, and consistent with the persistently increased bone remodeling exhibited by DMP1-caPTH1 mice crossed with LRP5 ^{-/-} or with DMP1-Sost mice, the osteoclast specific genes calcitonin receptor and TRAP remained elevated in DMP1-caPTH1;LRP5^{-/-} mice or in DMP1-caPTH1;DMP1-Sost mice (**Figure 7D**). Expression of the osteoclastogenic cytokines M-CSF and RANKL was increased in DMP1-caPTH1 mice; and their levels remained elevated, although not significantly for RANKL, in DMP1-caPTH1 mice crossed with LRP5 ^{-/-} or DMP1-Sost mice (**Figure 7C**). OPG expression, which was not different in DMP1-caPTH1 mice compared to WT littermates (**Figure 7C**), was lower in DMP1-caPTH1;LRP5^{-/-} mice or in DMP1-caPTH1;DMP1-Sost mice. This resulted in a higher RANKL/OPG ratio in animals expressing the DMP1-caPTH1 transgene and lacking LRP5 or overexpressing Sost.

Discussion

Early studies demonstrating localization of radiolabeled PTH in osteocytes and morphological changes in these cells upon hormonal treatment had suggested the regulation of osteocyte function by PTH ^(32,33). The findings that PTH decreases the expression of the osteocyte-derived inhibitor of bone formation sclerostin suggested a mechanism by which the hormone could increase bone mass through actions on osteocytes ^(23,24). More recently, we have shown that expression of a constitutively active mutant of the PTH receptor in osteocytes is sufficient to increase mass and remodeling in cancellous bone ⁽²⁵⁾. In the present report, we found that DMP1-caPTH1 mice exhibit accelerated bone formation on the periosteal and endocortical surfaces and increased intra-cortical remodeling, thereby demonstrating that PTH receptor signaling

in osteocytes governs periosteal bone formation and turnover also in cortical bone (**Figure 7E**). These actions of PTH receptor activation were observed in bones formed by either endochondral or intramembranous ossification. Moreover, higher periosteal apposition was found in both male and female mice regardless of the age of the animals, demonstrating that the effect of PTH receptor activation in osteocytes overrides the recognized action of growth as well as androgens on periosteal bone formation and size of long bones⁽³⁴⁾.

The current findings also demonstrate that the anabolic effect of PTH receptor signaling on the periosteal surface of cortical bone is dependent on inhibition of sclerostin expression, as it is abolished by overexpressing *Sost* in osteocytes. However, as judged by the persistent fluorochrome incorporation, bone formation coupled to the intracortical resorption exhibited by the DMP1-caPTHR1 mice was not decreased by removing LRP5 or overexpressing *Sost*. These findings suggest that sclerostin differentially regulates modeling-based periosteal bone formation versus remodeling-based endosteal bone formation. Further studies are warranted to specifically address the role of resorption on bone formation induced by PTH receptor signaling in osteocytes.

Expression of the endogenous (murine) *Sost* gene was lower in DMP1-caPTHR1 mice, regardless of whether the DMP1- (human) *Sost* transgene was co-expressed or not. This is consistent with earlier findings that PTH downregulates the expression of *Sost*/sclerostin *in vivo* and *in vitro*^(23,24) and with our previous report⁽²⁵⁾. Keller and colleagues demonstrated that inhibition of *Sost* expression by PTH is exerted through modulation of the transcription factor *Mef2c* via binding on the same distant regulatory

region of the *Sost* gene promoter that confers bone-specific expression of the gene ⁽³⁵⁾. Expression of the human *Sost* transgene in our DMP1-*Sost* mice is directed by the DMP1 promoter, not by the regulatory regions of the *Sost* gene. Therefore, the lower levels of human *Sost* mRNA observed in animals expressing both the DMP1-*Sost* and the DMP1-caPTH_R1 transgenes might result not from direct gene regulation by PTH_R activation but rather from changes either in osteocyte number or in their state of maturation. Nevertheless, even when human *Sost* mRNA expression was lower, human sclerostin protein was still detected at high levels in the double transgenic mice.

The mechanism by which sclerostin, the product of the *Sost* gene secreted by osteocytes, inhibits bone formation is not completely understood. However, the current knowledge indicates that sclerostin binds with high affinity to LRP6 and LRP5, transmembrane proteins that together with frizzled receptors mediate the actions of Wnt ligands. It is believed that sclerostin binding interferes with signaling downstream of these receptors thereby antagonizing the pro-differentiating and survival actions of Wnts on cells of the osteoblastic lineage ^(36,37). It was recently shown that sclerostin also associates with LRP4, another member of the LRP family of proteins ^(38,39); although its role in Wnt signaling is still uncertain. Nevertheless, it is possible that the remaining phenotypic features of PTH receptor activation in the absence of LRP5 in cortical bone demonstrated in this study, as well as cancellous bone in our previous study ⁽²⁵⁾, result from Wnt signaling through alternative LRPs.

Because the increase in bone mass exhibited by DMP1-caPTH_R1 mice is reduced in mice lacking LRP5, and a recent report indicated that LRP5 increases bone formation by inhibiting serotonin synthesis in the duodenum ⁽⁴⁰⁾, we examined whether the high

bone mass of the DMP1-caPTH_{R1} mice was associated with decreased intestinal expression of Tph1, the enzyme that controls serotonin synthesis. We found no significant changes in Tph1 expression in the duodenum, colon, or bone of DMP1-caPTH_{R1} compared to WT littermates (**Supplementary Figure 1**). Moreover, DMP1-Sost mice did not exhibit higher levels of Tph1 expression in either the intestine (or bone) as would be expected if the low bone mass in these mice was due to increased serotonin (**Supplementary Figure 1**). Consistent with our findings, Robling, Warman and colleagues have not detected changes in Tph1 in the intestine of the low bone mass LRP5^{-/-} mouse or in the high bone mass LRP5 G171V knock-in mouse⁽⁴¹⁾. Taken together, these findings are inconsistent with the involvement of gut-derived serotonin in the bone formation changes exhibited by DMP1-caPTH_{R1} mice with or without LRP5 deletion or Sost overexpression, and support the role of osteocyte-mediated regulation of the Wnt pathway on bone mass.

The higher periosteal BFR and cortical thickness exhibited by the DMP1-caPTH_{R1} mice contrast with the decreased periosteal BFR and thinner cortices found in mice in which the same active PTH receptor mutant is expressed under the control of the 2.3 fragment of the collagen 1a1 gene promoter (Col1a1-caPTH_{R1} mice), which is active not only in osteocytes but also in pre-osteoblasts and mature osteoblasts⁽⁴²⁾. Direct comparison of micro-CT images of calvarial bones of 4-week-old mice confirmed that indeed Col1a1-caPTH_{R1} mice exhibit decreased calvarial thickness whereas DMP1-caPTH_{R1} mice exhibit increased calvarial thickness compared to WT mice of the same age (**Supplementary Figure 3**). The divergent outcomes of activating the PTH receptor in different types of osteoblastic cells suggest that the positive effect on cortical bone

formation induced by PTH signaling in osteocytes is counter-balanced by simultaneous activation of PTH signaling in osteoblast precursors or mature osteoblasts. This antagonistic effect might result from direct inhibition of periosteal osteoblast differentiation by PTH receptor activation and it is consistent with the accumulation of immature osteoblasts with chronic elevation of PTH, such as in severe hyperparathyroidism ⁽⁴³⁾ or in the Col1a1-caPTHr1 transgenic mice ^(42,44). This phenomenon might also contribute to explain the failure of PTH to increase bone formation in the periosteal surface in some conditions ⁽¹⁷⁻¹⁹⁾.

The osteopenic phenotype of the DMP1-Sost transgenic mouse observed in vertebral cancellous bone is consistent with previous reports describing mice overexpressing human Sost under the control of the murine osteocalcin (OG-2) promoter ⁽⁴⁵⁾ or under the control of the regulatory regions of the Sost gene ⁽⁴⁶⁾. However, cortical bone volume in the femoral mid-diaphysis was not decreased in our DMP1-Sost mice up to 2 months of age. This is in agreement with the milder decrease in femoral BMD compared to lumbar vertebra observed in OG2-Sost mice by Winkler et al ⁽⁴⁵⁾. Future studies will be required to determine whether the phenotype of our DMP1-Sost animals becomes more prominent with age in both the axial and appendicular skeleton, as observed in 5-month-old human Sost mice in the study by Loots et al ⁽⁴⁶⁾.

In spite of the different effect of the Sost transgene by itself on cancellous versus cortical bone, Sost overexpression equally abolished the increase in bone mass and volume induced by the DMP1-caPTHr1 transgene in both bone envelopes. These findings confirm that the anabolic effect of PTH receptor signaling in osteocytes requires Sost/sclerostin downregulation. Sost overexpression converted the bone gain exhibited

by the DMP1-caPTH_{R1} mice into a bone loss in the DMP1-caPTH_{R1};DMP1-Sost mice. Thus, the double-transgenic mice exhibit reduced total, femoral or spinal BMD compared to animals expressing only the DMP1-Sost transgene, and a persistent increase in osteoclasts in the face of absent Wnt signaling and reduced expression of Wnt target genes and osteoblast markers. Similar effects were observed in DMP1-caPTH_{R1} mice lacking LRP5. OPG expression was not different in DMP1-caPTH_{R1} mice compared to WT littermates, likely due to opposing effects of PTH receptor signaling on the OPG gene, i.e. inhibition of transcription mediated by cAMP-response element-binding protein (CREB)⁽⁴⁷⁾ but stimulation of transcription mediated by elevated Wnt signaling^(48,49) (**Figure 7E, left panel**). However, OPG expression was markedly decreased in DMP1-caPTH_{R1} mice lacking LRP5^{-/-} or overexpressing Sost demonstrating that when Wnt signaling is reduced, the cAMP-dependent inhibition of OPG expression prevails (**Figure 7E, right panel**), resulting in higher RANKL/OPG ratio. This is particularly noticeable in the double transgenic DMP1-caPTH_{R1};DMP1-Sost mice in which resorption is exacerbated as evidenced by higher osteoclast number and calvarial marrow space compared to mice only expressing the caPTH_{R1} transgene. These observations, together with recent evidence demonstrating that deletion of β catenin-dependent canonical Wnt signaling in osteocytes leads to reduced levels of OPG and increased resorption⁽⁵⁰⁾, support a crucial role of osteocyte-derived OPG in bone resorption.

In closing, our study demonstrates that activation of PTH receptor signaling in osteocytes dictates the recognized actions of PTH on formation and resorption in cortical bone and defines the role of the Wnt pathway. Acceleration of periosteal bone

formation and apposition is due to downregulation of sclerostin, whereas the increase in osteoclast activity and intra-cortical remodeling is driven by osteocyte-dependent regulation of osteoclastogenic cytokines. Whether the mechanisms identified herein operate under conditions of endogenous elevation of PTH or administration of the hormone will require models of osteocyte-specific deletion of the PTH receptor. Our findings reveal that osteocytes are critical players in the regulation of cortical bone biology, opening new avenues to fracture prevention by targeting these most abundant bone cells.

Acknowledgements

The authors thank R. Lee, J.D. Benson, K. Vyas, and J.J. Goellner for technical assistance, Dr. Robyn Fuchs for guidance with imaging, Drs. Alex Robling and Matt Warman for sharing unpublished information, and Dr. David Burr for insightful discussions and critical reading of the manuscript.

Figure legends

Figure 1. Activation of PTHR1 signaling in osteocytes increases periosteal and endocortical bone formation. **(A)** Representative images of histologic sections showing calcein and alizarin double labeling in femoral mid-diaphyses from 4.6-week-old DMP1-caPTHR1 mice and WT littermates. **(B)** Static and dynamic histomorphometric measurements were performed in 3 male mice per group. Values are means \pm SD. * $p < 0.05$ versus WT mice.

Figure 2. Activation of PTHR1 signaling in osteocytes increases periosteal bone formation in calvaria and induces intra-cortical remodeling. Representative images of histologic sections showing calcein and alizarin double labeling in transverse sections taken 2 mm anterior to the junction between the fronto-parietal and sagittal sutures (indicated by the red line) from 4.6-week-old WT and DMP1-caPTHR1 mice (top). TRAPase staining of calvarial sections shows abundant osteoclasts in bones from DMP1-caPTHR1 mice (bottom). Bar indicates 50 μ m. Histomorphometric analysis was performed in the mid-third of one frontal bone excluding the area around the sutures. Periosteal BFR is the average of values of outer and inner periosteum. Calvarial marrow space was calculated by measuring histomorphometrically the area occupied by marrow versus bone in the mid-third of one frontal bone. Values are means \pm SD; $n = 3$ male mice per group. * $p < 0.05$ versus WT mice.

Figure 3. Periosteal bone formation induced by PTH receptor signaling in osteocytes is reduced in mice lacking LRP5. **(A)** Representative images of histologic sections show fluorochrome incorporation in femoral mid-diaphyses of 12-week-old WT and DMP1-caPTHR1 mice with or without LRP5. **(B)** Static and dynamic histomorphometric

measurements were determined in 3-4 male and female mice per group. Values are means \pm SD. * $p < 0.05$ versus respective controls without the DMP1-caPTH_{R1} transgene; # $p < 0.05$ versus DMP1-caPTH_{R1} mice.

Figure 4. The high bone mass phenotype of the DMP1-caPTH_{R1} mice is abolished by overexpression of Sost in osteocytes. **(A)** Expression of human or murine Sost was detected in ulnae lysates by quantitative PCR; n=3-5 female mice per group. ND, not detected. **(B)** Sclerostin expression was detected by immunohistochemistry in tibia using an anti-murine sclerostin antibody that also recognizes human sclerostin or using a specific anti-human sclerostin antibody. Bar indicates 10 μ m. **(C)** Total, femoral, and spinal BMD measured by DXA in 8-week-old mice expressing the DMP1-caPTH_{R1} and/or the DMP1-Sost transgenes, and WT littermates is shown; n=18-32 male and female mice per group. **(D)** Representative micro-CT images of cross-sections of femoral mid-diaphysis (upper panel) and L3 (lower panel) of WT and DMP1-caPTH_{R1} mice with or without DMP1-Sost transgene. Cortical bone area as a percentage of total area within the periosteal circumference (BA/TA) from the femoral diaphysis and trabecular BV/TV of the L3 body were measured in 4-7 male and female mice per group. Values represent the mean \pm SD. * $p < 0.05$ versus respective controls without the DMP1-caPTH_{R1} transgene; # $p < 0.05$ versus WT mice.

Figure 5. Periosteal bone formation induced by PTH receptor signaling in osteocytes is abolished by overexpression of Sost in osteocytes. **(A)** Representative images of histologic sections show fluorochrome incorporation in femoral mid-diaphyses of 10.5-week-old WT and DMP1-caPTH_{R1} mice with or without the DMP1-Sost transgene. **(B)**

Static and dynamic histomorphometric measurements were determined in 3-5 mice per group. Values are means \pm SD. * $p < 0.05$ versus WT mice.

Figure 6. The increased bone resorption induced by PTH receptor signaling in osteocytes persists in the absence of LRP5 and is exacerbated by Sost overexpression.

(A, B) TRAPase/von Kossa staining of calvarial sections and histomorphometric quantification of calvarial marrow space, expressed as the area occupied by marrow versus bone in the mid-third of one frontal bone, and osteoclasts, expressed as number per bone area. $n=4$ mice/group. Bar indicates 50 μm . **(C)** Osteocalcin and CTX were measured in plasma of 10.5-week-old DMP1-caPTH1 mice, with and without the DMP1-Sost transgene. Bars represent the mean \pm SD; $n=7-23$ mice per group. * $p < 0.05$ versus WT and LRP5^{-/-} or DMP1-Sost mice, respectively; # $p < 0.05$ versus DMP1-caPTH1 mice.

Figure 7. The increased expression of Wnt target genes and osteoblast markers induced by PTH receptor activation in osteocytes was obliterated by interfering with the Wnt pathway, but osteoclast markers were still elevated and OPG was markedly reduced. **(A-D)** Gene expression was measured by quantitative PCR. Results are expressed relative to the housekeeping gene ribosomal protein S2. Bars represent mean \pm SD of 4-5 mice per group. * $p < 0.05$ versus respective controls without the DMP1-caPTH1 transgene. **(E)** Schematic representation of the effects on cortical bone of PTH receptor signaling in osteocytes. Constitutive activation of PTH receptor in osteocytes (DMP1-caPTH1 mice) leads to cAMP-dependent Sost downregulation and increased Wnt signaling, which in turn stimulates periosteal bone formation. PTH receptor activation in osteocytes also increases RANKL expression and intra-cortical

remodeling. However, OPG expression is not affected, likely resulting from opposing effects on the expression of the gene by cAMP (reduction) and Wnts (elevation). When PTH receptor activation is combined with reduced Wnt signaling (LRP5 deficiency or Sost overexpression), the cAMP-mediated decrease in OPG prevails leading to markedly increased RANKL/OPG ratio and exacerbated bone resorption in the cortex.

Supplementary Figure 1. Expression of the hPTHr1 (A) and hSost (B) transgenes under the control of the DMP1-8kb-promoter and Tph1 expression in TG and WT littermate mice (C). Gene expression was measured by quantitative PCR. Results are expressed relative to the housekeeping gene ribosomal protein S2. Bars represent mean \pm SD of 3-7 mice per group. ND, not detected.

Supplementary Figure 2. The increased calvarial thickness and periosteal bone formation exhibited by the DMP1-caPTHr1 mice is reduced in the absence of LRP5 and is abolished by Sost overexpression. (A) Representative images showing calcein and alizarin double labeling in transverse sections of calvarial bones taken 2 mm anterior to the junction between the fronto-parietal and sagittal sutures from 12-week-old DMP1-caPTHr1 crossed with LRP5^{-/-} mice and 10.5-week-old DMP1-caPTHr1 crossed with DMP1-Sost mice, and respective littermate controls. (B and C) Histomorphometric analysis was performed in the mid-third of one frontal bone excluding the area around the sutures. Periosteal BFR is the average of values of outer and inner periosteal surface. Values are means \pm SD; n=3-5 mice per group. * p < 0.05 versus respective controls not expressing the DMP1-caPTHr1 transgene; # p < 0.05 versus DMP1-caPTHr1 mice.

Supplementary Figure 3. Calvarial thickness is higher in DMP1-caPTH_{R1} mice but lower in Col1a1-caPTH_{R1} mice compared to WT mice. Representative 2D micro-CT images of frontal bones from WT, Col1a1-caPTH_{R1} and DMP1-caPTH_{R1} mice. Average thickness measured in 3D-reconstructed image for each group is shown. Bar indicates 500 μm .

References

1. Ahlborg HG, Johnell O, Turner CH, Rannevik G, Karlsson MK 2003 Bone loss and bone size after menopause. *N Engl J Med* **349**:327-334.
2. Orwoll ES 2003 Toward an expanded understanding of the role of the periosteum in skeletal health. *J Bone Miner Res* **18**:949-954.
3. Crabtree N, Loveridge N, Parker M, Rushton N, Power J, Bell KL, Beck TJ, Reeve J 2001 Intracapsular hip fracture and the region-specific loss of cortical bone: analysis by peripheral quantitative computed tomography. *J Bone Miner Res* **16**:1318-1328.
4. Beck TJ, Ruff CB, Scott WW, Jr., Plato CC, Tobin JD, Quan CA 1992 Sex differences in geometry of the femoral neck with aging: a structural analysis of bone mineral data. *Calcif Tissue Int* **50**:24-29.
5. Duan Y, Seeman E, Turner CH 2001 The biomechanical basis of vertebral body fragility in men and women. *J Bone Miner Res* **16**:2276-2283.
6. Kalender WA, Felsenberg D, Louis O, Lopez P, Klotz E, Osteaux M, Fraga J 1989 Reference values for trabecular and cortical vertebral bone density in single and dual-energy quantitative computed tomography. *Eur J Radiol* **9**:75-80.
7. Allen MR, Hock JM, Burr DB 2004 Periosteum: biology, regulation, and response to osteoporosis therapies. *Bone* **35**:1003-1012.
8. Parfitt AM 2002 Parathyroid hormone and periosteal bone expansion. *J Bone Miner Res* **17**:1741-1743.
9. Christiansen P, Steiniche T, Brockstedt H, Mosekilde L, Hessov I, Melsen F 1993 Primary hyperparathyroidism: iliac crest cortical thickness, structure, and remodeling evaluated by histomorphometric methods. *Bone* **14**:755-762.
10. Lindsay R, Zhou H, Cosman F, Nieves J, Dempster DW, Hodsmann AB 2007 Effects of a one-month treatment with parathyroid hormone (1-34) on bone formation on cancellous, endocortical and periosteal surfaces of the human ilium. *J Bone Miner Res* **22**:495-502.
11. Kneissel M, Boyde A, Gasser JA 2001 Bone tissue and its mineralization in aged estrogen-depleted rats after long-term intermittent treatment with parathyroid hormone (PTH) analog SDZ PTS 893 or human PTH(1-34). *Bone* **28**:237-250.

12. Iida-Klein A, Lu SS, Cosman F, Lindsay R, Dempster DW 2007 Effects of cyclic vs. daily treatment with human parathyroid hormone (1-34) on murine bone structure and cellular activity. *Bone* **40**:391-398.
13. Jilka RL, O'Brien CA, Ali AA, Roberson PK, Weinstein RS, Manolagas SC 2009 Intermittent PTH stimulates periosteal bone formation by actions on post-mitotic preosteoblasts. *Bone* **44**:275-286.
14. Hirano T, Burr DB, Cain RL, Hock JM 2000 Changes in geometry and cortical porosity in adult, ovary-intact rabbits after 5 months treatment with LY333334 (hPTH 1-34). *Calcif Tissue Int* **66**:456-460.
15. Bikle DD, Sakata T, Leary C, Elalieh H, Ginzinger D, Rosen CJ, Beamer W, Majumdar S, Halloran BP 2002 Insulin-like growth factor I is required for the anabolic actions of parathyroid hormone on mouse bone. *J Bone Miner Res* **17**:1570-1578.
16. Miyakoshi N, Kasukawa Y, Linkhart TA, Baylink DJ, Mohan S 2001 Evidence that anabolic effects of PTH on bone require IGF-I in growing mice. *Endocrinology* **142**:4349-4356.
17. Recker RR, Bare SP, Smith SY, Varela A, Miller MA, Morris SA, Fox J 2009 Cancellous and cortical bone architecture and turnover at the iliac crest of postmenopausal osteoporotic women treated with parathyroid hormone 1-84. *Bone* **44**:113-119.
18. Fox J, Miller MA, Newman MK, Recker RR, Turner CH, Smith SY 2007 Effects of daily treatment with parathyroid hormone 1-84 for 16 months on density, architecture and biomechanical properties of cortical bone in adult ovariectomized rhesus monkeys. *Bone* **41**:321-330.
19. Burr DB, Hirano T, Turner CH, Hotchkiss C, Brommage R, Hock JM 2001 Intermittently administered human parathyroid hormone(1-34) treatment increases intracortical bone turnover and porosity without reducing bone strength in the humerus of ovariectomized cynomolgus monkeys. *J Bone Miner Res* **16**:157-165.
20. Jilka RL, Weinstein RS, Bellido T, Roberson P, Parfitt AM, Manolagas SC 1999 Increased bone formation by prevention of osteoblast apoptosis with parathyroid hormone. *J Clin Invest* **104**:439-446.
21. Bellido T, Ali AA, Plotkin LI, Fu Q, Gubrij I, Roberson PK, Weinstein RS, O'Brien CA, Manolagas SC, Jilka RL 2003 Proteasomal degradation of Runx2 shortens parathyroid hormone-induced anti-apoptotic signaling in osteoblasts. A putative explanation for why intermittent administration is needed for bone anabolism. *J Biol Chem* **278**:50259-50272.

22. Jilka RL 2007 Molecular and cellular mechanisms of the anabolic effect of intermittent PTH. *Bone* **40**:1434-1446.
23. Keller H, Kneissel M 2005 SOST is a target gene for PTH in bone. *Bone* **37**:148-158.
24. Bellido T, Ali AA, Gubrij I, Plotkin LI, Fu Q, O'Brien CA, Manolagas SC, Jilka RL 2005 Chronic elevation of PTH in mice reduces expression of sclerostin by osteocytes: a novel mechanism for hormonal control of osteoblastogenesis. *Endocrinology* **146**:4577-4583.
25. O'Brien CA, Plotkin LI, Galli C, Goellner J, Gortazar AR, Allen MR, Robling AG, Bouxsein M, Schipani E, Turner CH, Jilka RL, Weinstein RS, Manolagas SC, Bellido T 2008 Control of bone mass and remodeling by PTH receptor signaling in osteocytes. *PLoS ONE* **3**:e2942.
26. Kalajzic I, Braut A, Guo D, Jiang X, Kronenberg MS, Mina M, Harris MA, Harris SE, Rowe DW 2004 Dentin matrix protein 1 expression during osteoblastic differentiation, generation of an osteocyte GFP-transgene. *Bone* **35**:74-82.
27. Clement-Lacroix P, Ai M, Morvan F, Roman-Roman S, Vayssiere B, Belleville C, Estrera K, Warman ML, Baron R, Rawadi G 2005 Lrp5-independent activation of Wnt signaling by lithium chloride increases bone formation and bone mass in mice. *Proc Natl Acad Sci U S A* **102**:17406-17411.
28. Erlebacher A, Derynck R 1996 Increased expression of TGF-beta 2 in osteoblasts results in an osteoporosis-like phenotype. *J Cell Biol* **132**:195-210.
29. Parfitt AM, Drezner MK, Glorieux FH, Kanis JA, Malluche H, Meunier PJ, Ott SM, Recker RR 1987 Bone histomorphometry: standardization of nomenclature, symbols, and units. *J Bone Min Res* **2**:595-610.
30. Li X, Zhang Y, Kang H, Liu W, Liu P, Zhang J, Harris SE, Wu D 2005 Sclerostin binds to LRP5/6 and antagonizes canonical Wnt signaling. *J Biol Chem* **280**:19883-19887.
31. Robinson JA, Chatterjee-Kishore M, Yaworsky PJ, Cullen DM, Zhao W, Li C, Kharode Y, Sauter L, Babij P, Brown EL, Hill AA, Akhter MP, Johnson ML, Recker RR, Komm BS, Bex FJ 2006 WNT/beta-catenin signaling is a normal physiological response to mechanical loading in bone. *J Biol Chem* **281**:31720-31728.
32. Neuman WF, Neuman MW, Sammon PJ, Casarett GW 1975 The metabolism of labeled parathyroid hormone. IV. Autoradiographic studies. *Calcif Tissue Res* **18**:263-270.

33. Parfitt AM 1976 The actions of parathyroid hormone on bone: relation to bone remodeling and turnover, calcium homeostasis, and metabolic bone diseases. II. PTH and bone cells: bone turnover and plasma calcium regulation. *Metabolism* **25**:909-955.
34. Seeman E 2002 Pathogenesis of bone fragility in women and men. *Lancet* **359**:1841-1850.
35. Leupin O, Kramer I, Collette NM, Loots GG, Natt F, Kneissel M, Keller H 2007 Control of the SOST bone enhancer by PTH using MEF2 transcription factors. *J Bone Miner Res* **22**:1957-1967.
36. Glass DA, Karsenty G 2007 In vivo analysis of Wnt signaling in bone. *Endocrinology* **148**:2630-2634.
37. Baron R, Rawadi G 2007 Targeting the Wnt/beta-catenin pathway to regulate bone formation in the adult skeleton. *Endocrinology* **148**:2635-2643.
38. Choi HY, Dieckmann M, Herz J, Niemeier A 2009 Lrp4, a novel receptor for dickkopf 1 and sclerostin, is expressed by osteoblasts and regulates bone growth and turnover in vivo. *PLoS ONE* **4**:e7930.
39. Li Y, Pawlik B, Elcioglu N, Aglan M, Kayserili H, Yigit G, Percin F, Goodman F, Nurnberg G, Cenani A, Urquhart J, Chung BD, Ismail S, Amr K, Aslanger AD, Becker C, Netzer C, Scambler P, Eyaid W, Hamamy H, Clayton-Smith J, Hennekam R, Nurnberg P, Herz J, Temtamy SA, Wollnik B 2010 LRP4 Mutations Alter Wnt/beta-Catenin Signaling and Cause Limb and Kidney Malformations in Cenani-Lenz Syndrome. *Am J Hum Genet* **86**:696-706.
40. Yadav VK, Ryu JH, Suda N, Tanaka KF, Gingrich JA, Schutz G, Glorieux FH, Chiang CY, Zajac JD, Insogna KL, Mann JJ, Hen R, Ducy P, Karsenty G 2008 Lrp5 controls bone formation by inhibiting serotonin synthesis in the duodenum. *Cell* **135**:825-837.
41. Warman M 2010 Regulation of bone mass by direct action of LRP5 in bone. *Proceedings of the 2010 ASBMR Annual Meeting*: pg 269.
42. Calvi LM, Sims NA, Hunzelman JL, Knight MC, Giovannetti A, Saxton JM, Kronenberg HM, Baron R, Schipani E 2001 Activated parathyroid hormone/parathyroid hormone-related protein receptor in osteoblastic cells differentially affects cortical and trabecular bone. *J Clin Invest* **107**:277-286.
43. Pyrah LN, Hodgkinson A, Anderson CK 1966 Primary hyperparathyroidism. *Br J Surg* **53**:245-316.
44. Calvi LM, Shin HI, Knight MC, Weber JM, Young MF, Giovannetti A, Schipani E 2004 Constitutively active PTH/PTHrP receptor in odontoblasts alters

odontoblast and ameloblast function and maturation. *Mech Dev* **121**:397-408.

45. Winkler DG, Sutherland MK, Geoghegan JC, Yu C, Hayes T, Skonier JE, Shpektor D, Jonas M, Kovacevich BR, Staehling-Hampton K, Appleby M, Brunkow ME, Latham JA 2003 Osteocyte control of bone formation via sclerostin, a novel BMP antagonist. *EMBO J* **22**:6267-6276.
46. Loots GG, Kneissel M, Keller H, Baptist M, Chang J, Collette NM, Ovcharenko D, Plajzer-Frick I, Rubin EM 2005 Genomic deletion of a long-range bone enhancer misregulates sclerostin in Van Buchem disease. *Genome Res* **15**:928-935.
47. Fu Q, Jilka RL, Manolagas SC, O'Brien CA 2002 Parathyroid hormone stimulates receptor activator of NFkappa B ligand and inhibits osteoprotegerin expression via protein kinase A activation of CREB. *J Biol Chem* **277**:48868-48875.
48. Glass DA, Bialek P, Ahn JD, Starbuck M, Patel MS, Clevers H, Taketo MM, Long F, McMahon AP, Lang RA, Karsenty G 2005 Canonical Wnt signaling in differentiated osteoblasts controls osteoclast differentiation. *Dev Cell* **8**:751-764.
49. Holmen SL, Zylstra CR, Mukherjee A, Sigler RE, Faugere MC, Bouxsein ML, Deng L, Clemens TL, Williams BO 2005 Essential role of beta-catenin in postnatal bone acquisition. *J Biol Chem* **280**:21162-21168.
50. Kramer I, Halleux C, Keller H, Pegurri M, Gooi JH, Weber PB, Feng JQ, Bonewald LF, Kneissel M 2010 Osteocyte Wnt/beta-catenin signaling is required for normal bone homeostasis. *Mol Cell Biol* **30**:3071-3085.

Figure 1.

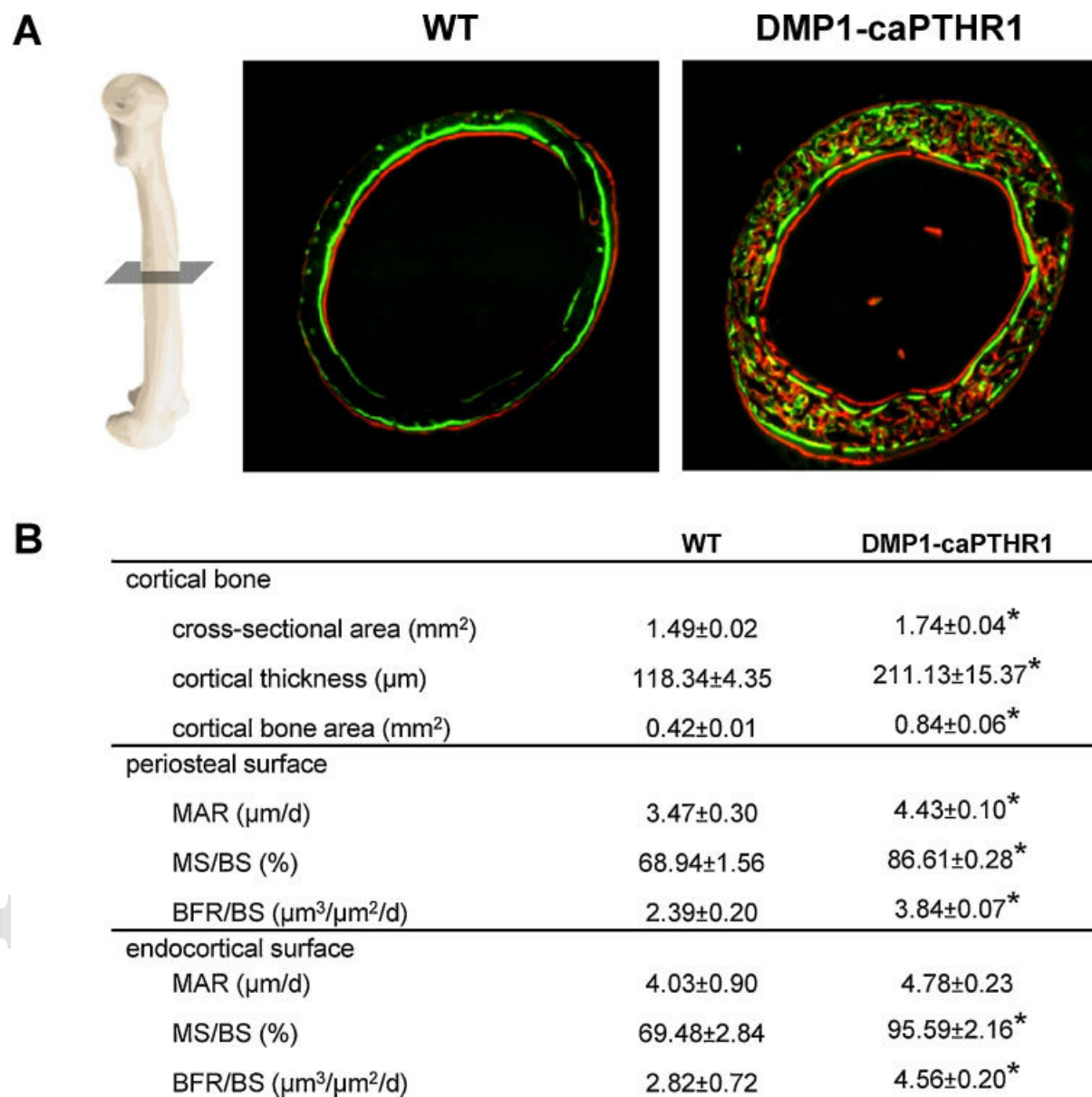


Figure 2.

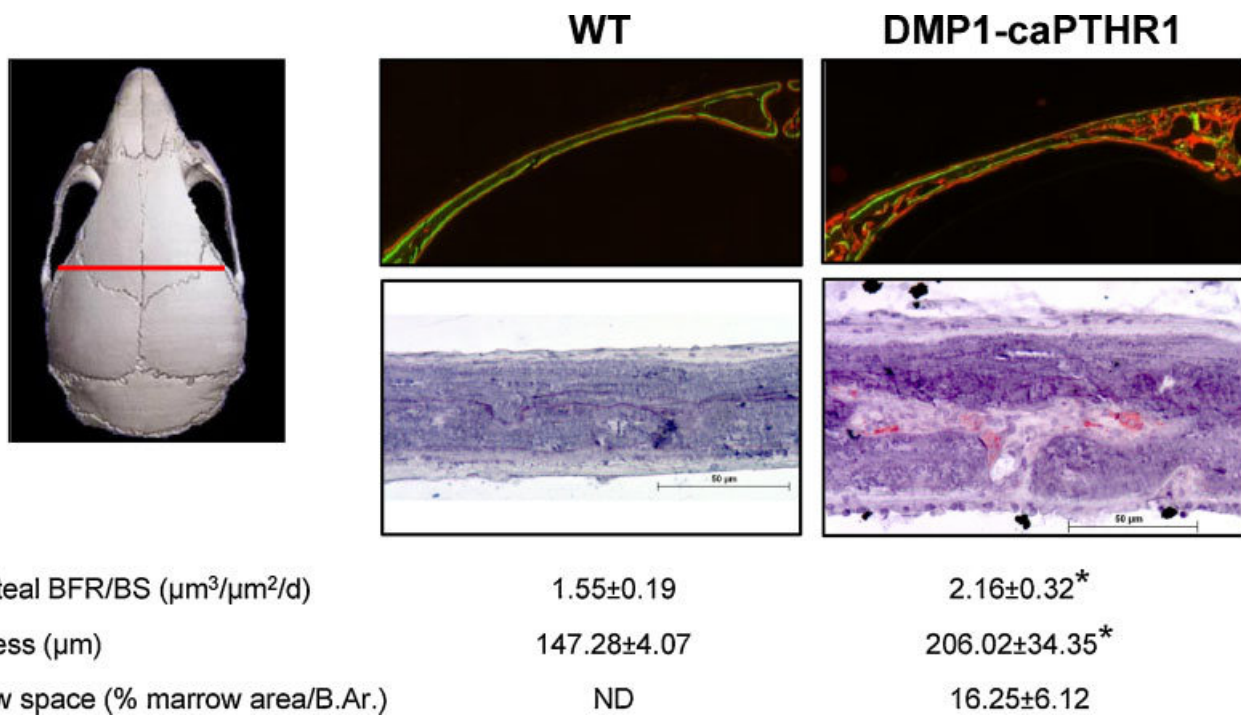


Figure 3.

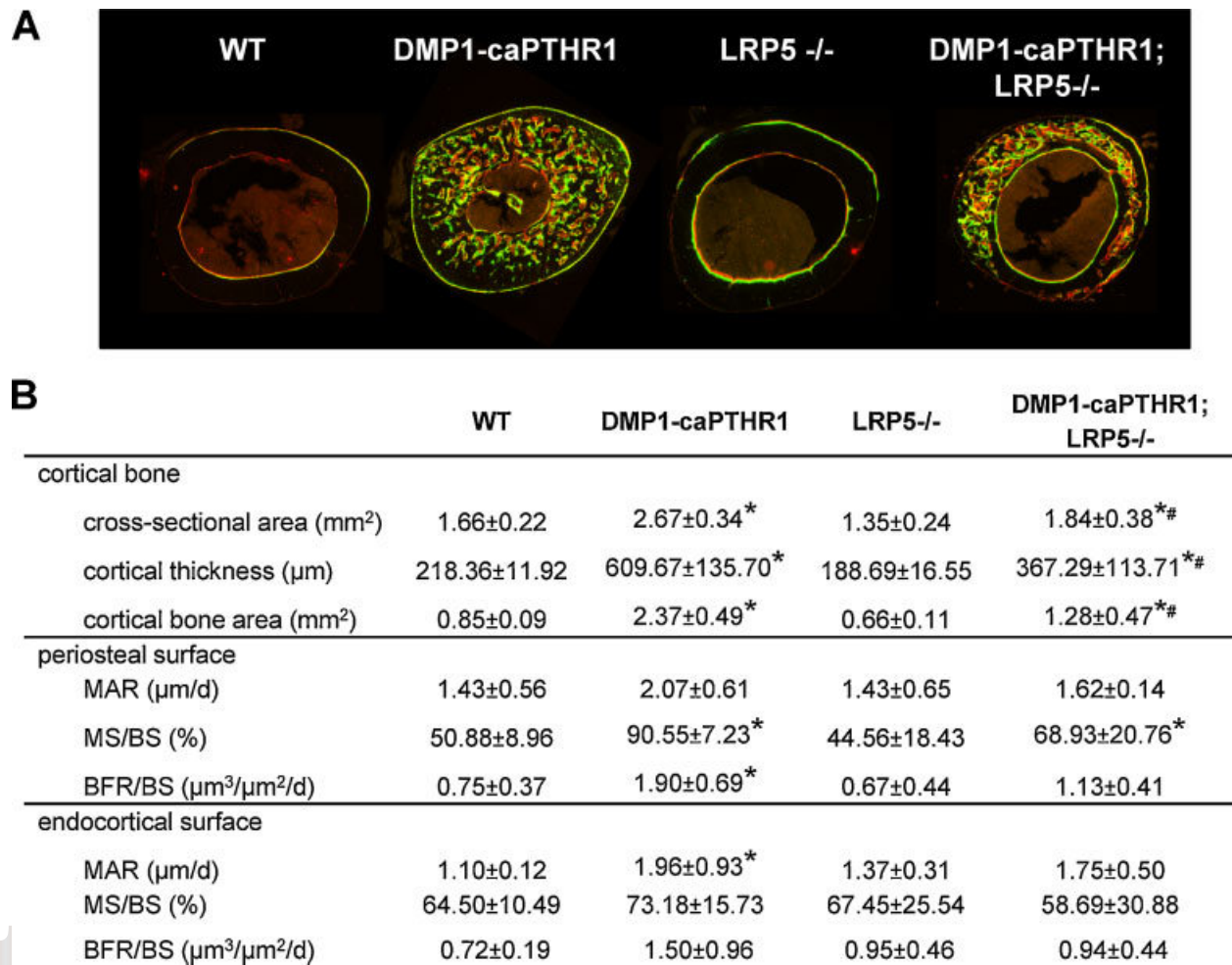


Figure 4.

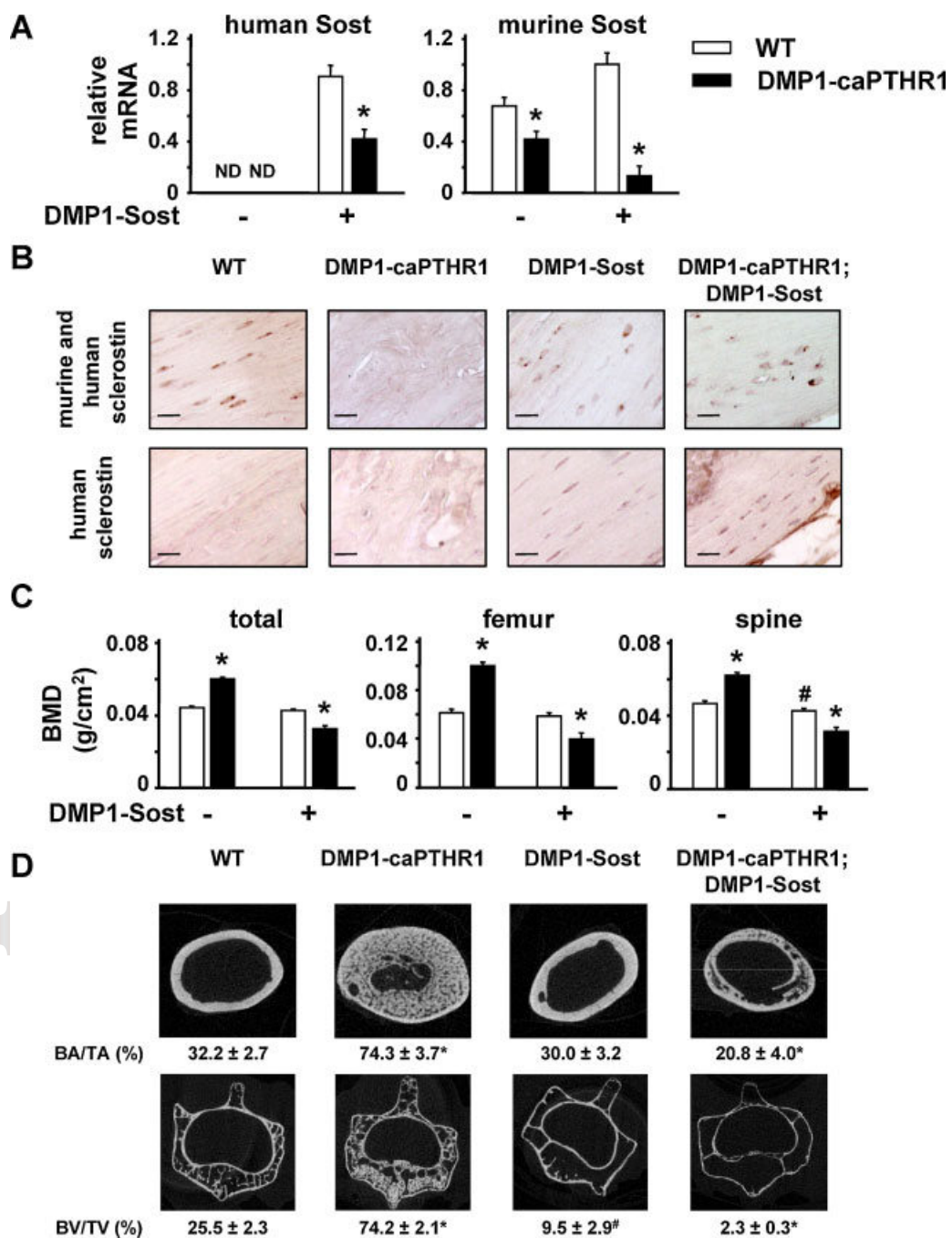


Figure 5.

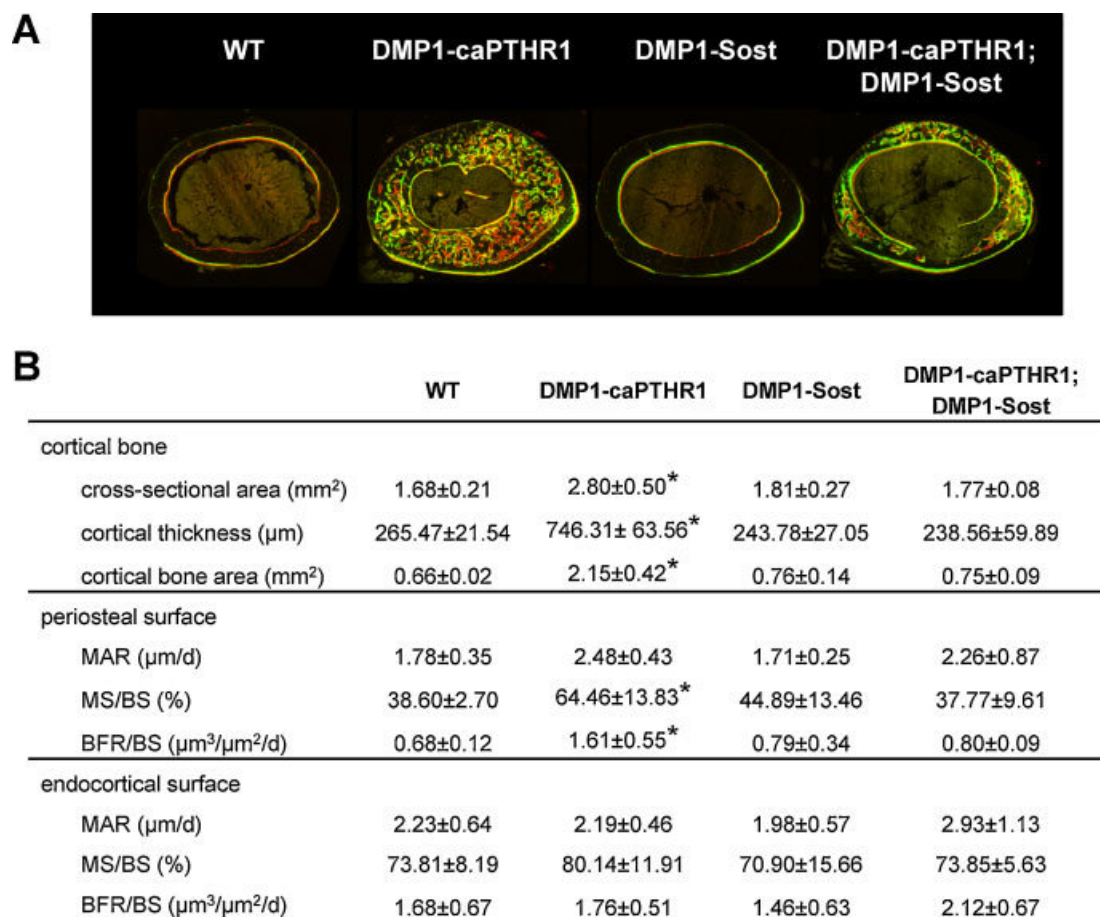


Figure 6.

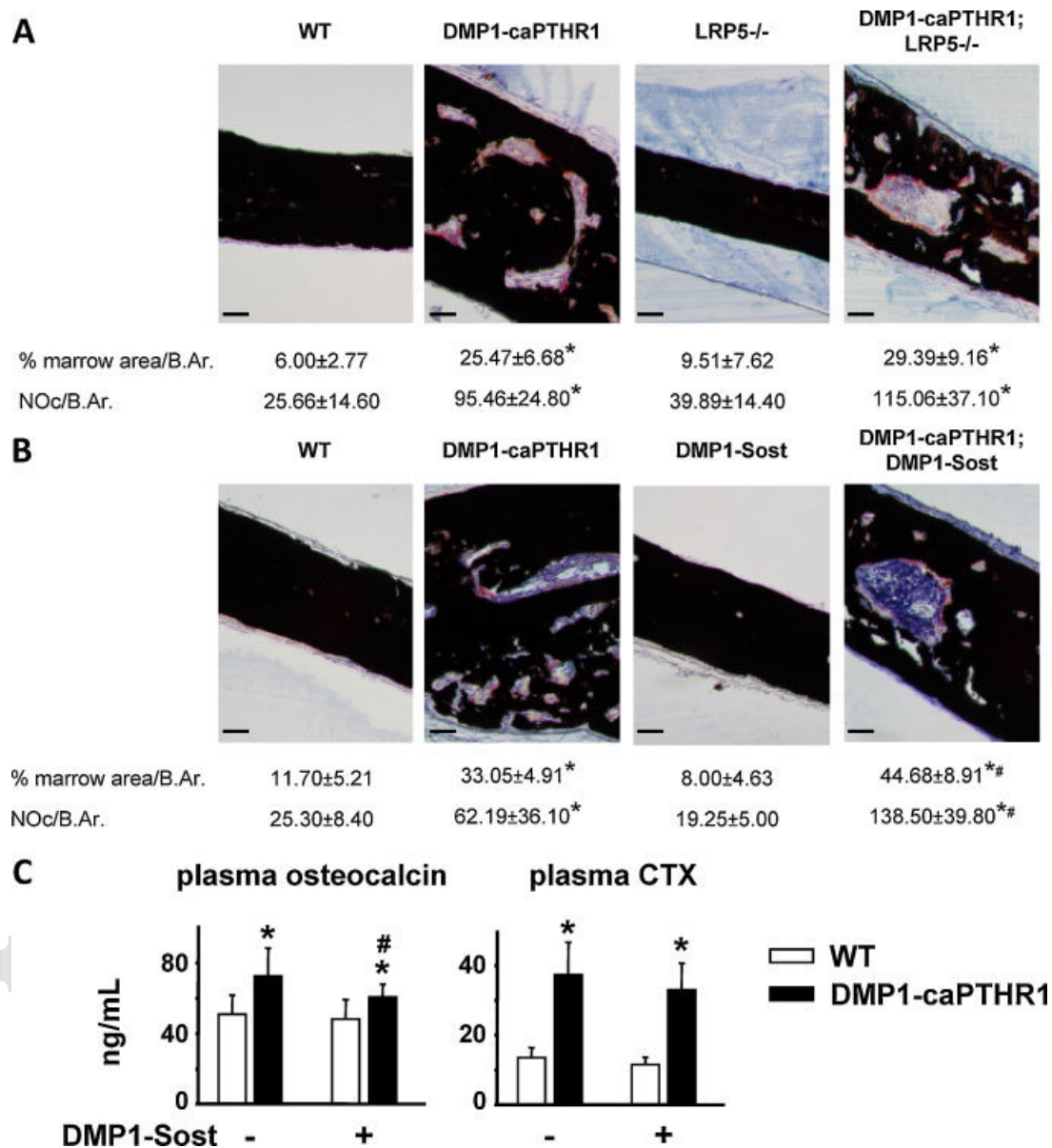


Figure 7.

